arXiv:1105.4051v2 [cond-mat.mtrl-sci] 24 Jul 2011

Nonlinear bias dependence of spin-transfer torque from atomic first principles

Xingtao Jia[1], Ke Xia[1], Youqi Ke[2] and Hong Guo[2]
[1] *Department of Physics, Beijing Normal University, Beijing 100875, China*
[2] *Centre for the Physics of Materials and Department of Physics,*
McGill University, Montreal, PQ, H3A 2T8, Canada
(Dated: January 21, 2013)

We report first-principles analysis on the bias dependence of spin-transfer torque (STT) in Fe/MgO/Fe magnetic tunnel junctions. The in-plane STT changes from linear to nonlinear dependence as the bias voltage is increased from zero. The angle dependence of STT is symmetric at low bias but asymmetric at high bias. The nonlinear behavior is marked by a threshold point in the STT versus bias curve. The high-bias nonlinear STT is found to be controlled by a resonant transmission channel in the anti-parallel configuration of the magnetic moments. Disorder scattering due to oxygen vacancies in MgO significantly changes the STT threshold bias.

PACS numbers: 72.25.Ba, 72.10.Bg, 85.75.-d

I. INTRODUCTION

Magnetic tunnel junction (MTJ) has attracted great attention due to its importance in magnetic random-access memory (MRAM) and read-sensor technology. A basic MTJ is made of two ferromagnetic (FM) layers sandwiching a thin insulating material. Digital information is coded by magnetic moments of the FM layer being in parallel or anti-parallel configurations (PC or APC). In commercial MRAMs, switching between PC and APC is achieved by external magnetic fields. An emerging trend is to switch by spin-transfer torque (STT) predicted theoretically[1] and demonstrated experimentally[2–4] where a spin-polarized current transfers angular momentum to a FM layer causing magnetic moment reversal. STT holds great promise to simplify the MRAM structure, down-scale device size, and reduce power consumption.

One of the most important issues concerning STT is its dependence on external bias voltage V_b that drives the spin-polarized current in the first place. Understanding this issue is rather difficult not only because torque is a vector[5–9] but also because STT operates at nonequilibrium due to the flow of spin currents. A physical picture concerning the bias dependence of STT, from the linear to nonlinear bias regime, is yet to be established from atomic first principles. Theoretically, V_b dependence of STT was investigated by model analysis such as the tight-binding model[10,11] and free-electron model.[12–14] More recently, Heiliger and Stiles[15] analyzed STT for an MgO based MTJ based on equilibrium electronic structure obtained from density-functional theory (DFT). The in-plane STT was calculated[15] up to $V_b = \pm 0.5$ V and showed essentially a linear dependence on V_b, and the out-of-plane STT was found to be quadratic in V_b, which is consistent with tight-binding[10] and experimental results.[5,16]

Existing calculations provided valuable understanding of STT at the small V_b regime. To establish a complete picture, it is important to investigate STT at higher bias from atomic first principles. Indeed, recent experimental data[8] already showed a strong nonlinear V_b dependence of in-plane STT, and observable non-quadratic out-of-plane STT beyond $V_b \approx 0.2$V. It is the purpose of this work to report a first-principles analysis of STT in the most technologically important Fe/MgO/Fe MTJ from low- to high-bias regimes, focusing on its nonlinear V_b dependence. We found that the in-plane STT changes from linear to nonlinear dependence as V_b is increased from zero. The angle dependence of STT is symmetric at low bias but asymmetric at high bias. The nonlinear behavior is marked by a threshold point in the STT versus bias curve which is controlled by a resonant transmission channel in the APC current. We also found that the nonlinear STT is affected by atomic defects−oxygen vacancies in MgO−hence, in principle, can be tuned by interface engineering. Results are compared to the corresponding experimental data.

This paper is organized as follows. In Sec. II, we give the details of our calculation based on Keldysh nonequilibrium Green's function (NEGF) and wave-function-matching function method. In Sec. III, we present our results on Fe/MgO/Fe(001) MTJs with clean and disordered interfaces. Section IV is our summary.

II. ELECTRONIC STRUCTURE AND TRANSPORT CALCULATION

The MTJ we consider consists of an MgO barrier sandwiched by two semi-infinite Fe leads shown in Fig.1. The system is periodic in the x-z plane and current flows along y corresponding to the (001) material-growth direction. A very small lattice mismatch between Fe and MgO is neglected by fixing the interfacial atoms at their bulk bcc positions. Our calculation is from first principles where DFT is carried out within the Keldysh nonequilibrium Green's function (NEGF) method.[17,18] Here, DFT determines the Hamiltonian of the open device structure, and NEGF determines the nonequilibrium statistics of the device operation and the nonequilibrium density matrix. The NEGF-DFT is solved self-consistently under finite bias during current flow. For devices hav-

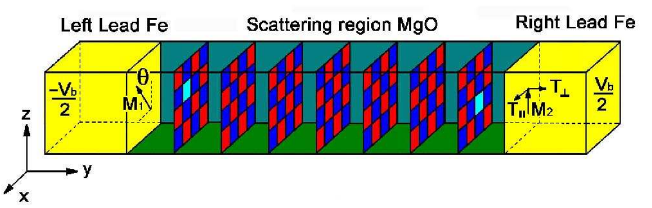

FIG. 1: (Color online) Sketch of a Fe/MgO/Fe(001) MTJ having seven MgO layers. The magnetization of the left Fe lead ($\mathbf{M}_1$) is fixed and that of the right Fe lead ($\mathbf{M}_2$) is free to rotate. $\mathbf{M}_2$ is pointing along the z axis; $\mathbf{M}_1$ lies in the x-z plane, the angle θ is the angle between $\mathbf{M}_1$ and $\mathbf{M}_2$. The red and blue grids in the scattering region (MgO) denote the O and Mg atoms, respectively. There may be some interfacial disorder (oxygen vacancy, cyan grid) at the Fe/MgO interfaces. The applied bias eV_b=$\mu_R - \mu_L$, where μ_R and μ_L are chemical potentials of the right and left leads.

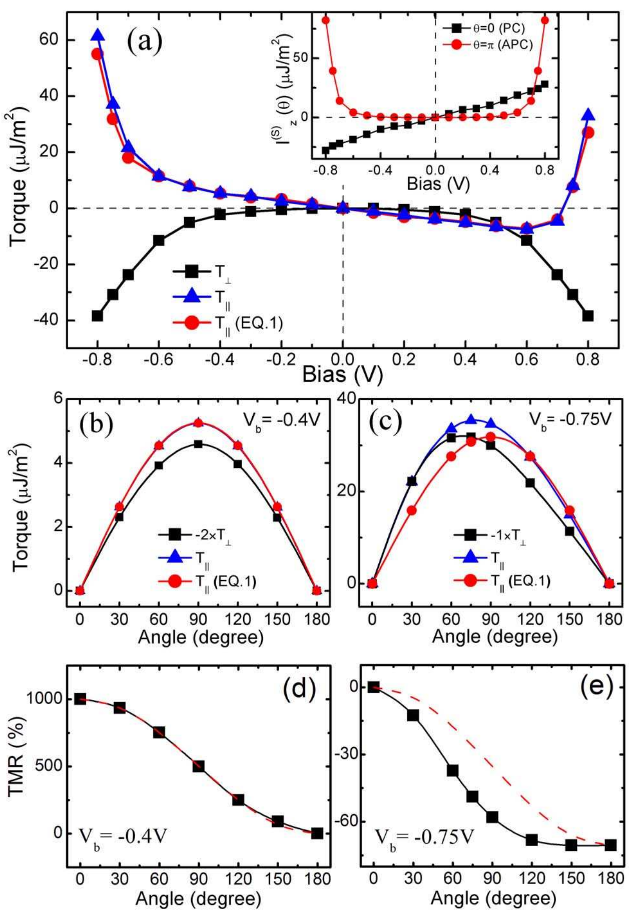

FIG. 2: (Color online) (a) STT of ideal Fe/MgO(7L)/Fe with angle $\theta = 90^o$ between $\mathbf{M}_1$ and $\mathbf{M}_2$. Black squares and red circles are out-of-plane and in-plane STT calculated by the wave-function-matching method, respectively, the blue up-triangle is the in-plane STT calculated by Eq. (1). Inset: spin currents in PC and APC. (b) and (c): angular dependence of STT at $V_b = -0.4$, and -0.75 V, respectively. (d) and (e): angular dependence of TMR at $V_b = -0.4$, and-0.75 V, respectively; the red dash lines are standard cosine-dependence TMR according to Ref. 26.

ing oxygen vacancies (OV, the most energetic favorable defects), we further apply the nonequilibrium-vertex-correction (NVC) theory[18] for disorder averaging at both the nonequilibrium-density-matrix level and transport-calculation level. The NEGF-DFT-NVC formalism allows one to self-consistently calculate quantum transport properties from atomic first principles without phenomenological parameters. We refer interested readers to the original work.[18]

Moreover, The self-consistent nonequilibrium potentials were used as input to a TB-MTO wave-function-matching calculation. The scattering wave functions of the whole system were obtained explicitly. Because we cannot embody the nonequilibrium NVC into the out-of-plane STT calculations at present, a supercell is used to assess out-of-plane STT in the presence of interfacial disorder. In the calculations, an 800 × 800 k-mesh is used to sample the two-dimensional Brillouin zone (BZ) in the x-z plane (see Fig. 1) to ensure accurate convergence. Other numerical details are similar to those of Ref. 19 and 20.

To check our electronic structure of Fe/MgO/Fe, we calculate the zero-bias TMR for 7 monolayers (ML) MgO barrier, which is 5100% with the perfect Fe/MgO interface while decreases dramatically to 350% (78%) with 3% (7%) OV at both interfaces. The TMR of a clean junction is consistent with the published first-principles calculation,[21] while the TMR of junctions with vacancies are in the range of experimental measurement.[22–24] The results indicate that we have got the right electronic structure.

III. BIAS DEPENDENCE OF STT

Before presenting results, let's consider some general trends. Neglecting any spin dependent scattering in the tunnel barrier, the in-plane STT can be obtained from conservation of spin current,[10]

$$\mathbf{T}_{||}(\theta) = \frac{I_z^{(s)}(\pi) - I_z^{(s)}(0)}{2}\mathbf{M_2} \times (\mathbf{M_1} \times \mathbf{M_2}) \qquad (1)$$

where θ is the relative angle between magnetization $\mathbf{M}_1$ and $\mathbf{M}_2$ (see Fig. 1). $I_z^{(s)}(0) \equiv \frac{\hbar}{2e}[I^\uparrow(0) - I^\downarrow(0)]$ is the spin-polarized current density in PC and $I_z^{(s)}(\pi) \equiv \frac{\hbar}{2e}[I^\uparrow(\pi) - I^\downarrow(\pi)]$ is that of APC. By structural symmetry, $I_z^{(s)}(0)$ should be an odd function and $I_z^{(s)}(\pi)$ an even function of V_b. Hence, at not too large V_b, we can write $I_z^{(s)}(0) \approx \gamma_1 V_b$ and $I_z^{(s)}(\pi) \approx \gamma_2 V_b^2$, where γ_1 and γ_2 are constants. From these considerations, Eq. (1) suggests $I_z^{(s)}(0)$ to dominate $T_{||}$ at small V_b (positive V_b) while $I_z^{(s)}(\pi)$ to dominate at higher V_b. Hence, $T_{||}$ should start from a linear dependence and turn into a nonlinear dependence as V_b is increased; the turning point defines a "threshold" bias whose value is determined roughly by the material-specific constants $\gamma_{1,2}$. At low bias, the out-of-plane STT demonstrates a simple quadratic relation[10] that we can write as $T_\perp = \gamma_\perp V_b^2$.

After the NEGF-DFT self-consistent calculation is converged,[18] spin currents $I^\uparrow$ and $I^\downarrow$ can be calculated by NEGF[18] and the in-plane STT $T_{||}$ obtained from Eq. (1). The out-of-plane STT $T_\perp$ (also $T_{||}$) can be obtained from a scattering-wave-function approach following Ref. 19. Figure 2 shows plots of the calculated $T_{||}$ and $T_\perp$ versus V_b for a perfect Fe/MgO/Fe MTJ (no disorder) having seven layers of MgO, where magnetization $\mathbf{M}_1 \perp \mathbf{M}_2$, *i.e.,* $\theta = 90^o$ (see Fig. 1). Seven-layer MgO is used because it is the thickness of experimental device[16] with which we shall compare results (see below). The blue (up-triangle, $T_{||}$) and black (solid square, $T_\perp$) curves were calculated from the scattering wave functions.[19] The red curve (solid circle, $T_{||}$) was calculated from Eq. (1), which agrees with the blue curve very well at least for lower V_b.[25] At lower bias up to ±0.5V, $T_{||}$ is linear in V_b and it is in agreement with Ref.15. As V_b increases, $T_{||}$ becomes gradually nonlinear and a clear threshold at $V_b \sim 0.65$V (e.g., turning point of the curves) is seen, as expected from the general considerations discussed above.

The inset of Fig. 2(a) plots the spin-current density versus V_b. Spin-polarized current density $I_z^{(s)}(0)$ is indeed linear in V_b whose slope is $\gamma_1 \approx 35\mu\mathrm{JV}^{-1}\mathrm{m}^{-2}$. Spin-polarized current density $I_z^{(s)}(\pi)$ is, as expected, an even function of V_b and, by fitting to a quadratic form $\gamma_2 V_b^2$, we found that $\gamma_2 \approx 5\mu\mathrm{JV}^{-2}\mathrm{m}^{-2}$ for $V_b \leq 0.5$ V. The small value of γ_2 makes $I_z^{(s)}(\pi)$ to have a very weak V_b dependence, until its sudden increase at $V_b \sim 0.6$ V, resulting in the threshold of $T_{||}$ at $\sim$0.65 V.

The out-of-plane STT shows quadratic behavior at the lower bias with $\gamma_\perp \approx -13\mu\mathrm{JV}^{-2}\mathrm{m}^{-2}$, and it is very close to the published calculated value of $-14\mu\mathrm{JV}^{-2}\mathrm{m}^{-2}$ with a six-ML MgO barrier.[15] Quantitatively, $T_\perp < T_{||}$ for $V_b < 0.5$ V but reaches a similar scale when $V_b > 0.5$ V.

Not only the bias dependence of STT [see Fig. 2(a)] is changed by the sudden increase of APC current $I_z^{(s)}(\pi)$, the angular dependence of STT is also modified. As shown in Fig. 2(b), the angular dependence behaves as sinθ at a small bias $V_b = -0.4$ V. It however deviates from the sine dependence at a higher bias $V_b = -0.75$ V [see Fig. 2(c)]. Experimental evidence of asymmetric angular-dependent STT at higher bias had been already observed before.[16]

Can the angular dependence of in-plane STT be understood by the angular dependence of the charge current or TMR? We give the angular dependence of TMR at a small bias $V_b = -0.4$ V [see Fig. 2(d)], and a large bias $V_b = -0.75$ V [see Fig.2(e)]. The angular dependence of TMR at low bias follows the cosine function[26] and deviates from the cosine function at high bias. At high bias, the in-plane STT shows an asymmetry and the peak is close to the parallel side, while the angular-resolved TMR decreases always faster than cosine function as the magnetization goes from parallel to antiparallel. Notice here, we have negative TMR at high bias. So, the angular dependence of TMR cannot explain our calculated angular dependence of in-plane STT.

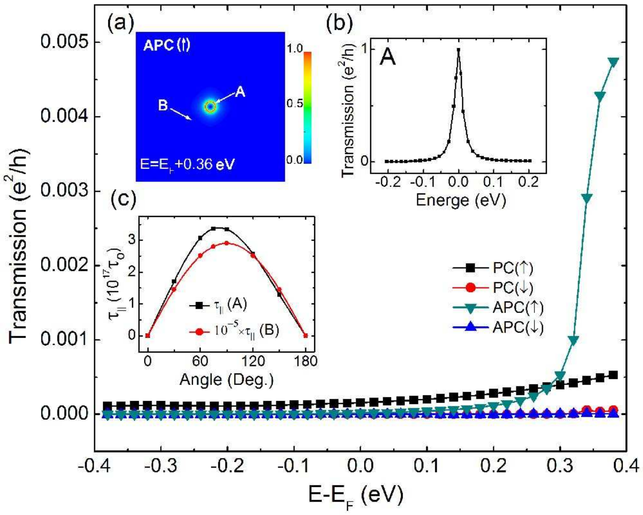

FIG. 3: (Color online) Energy dependent spin polarized transmission coefficient of ideal Fe/MgO(7L)/Fe MTJ at $V_b = \pm 0.75$V. Insert (a): the $\mathbf{k}_{||}$ resolved transmission hot spot of the ↑ -channel in APC at energy E=E$_F$+0.36eV. Insert (b): the energy dependent transmission of a bright point A on the ring of the insert (a) at k$_x$=k$_y$=0.278Å^{-1}. Insert (c): angular dependent in-plane STT at resonant point A k$_x$=k$_y$= 0.278Å^{-1}, and normal point B k$_x$=k$_y$= -1.624Å^{-1} of the insert (a); therein, $\tau_o \equiv \frac{\hbar}{2e} k\Omega^{-1} m^{-2}$ sets the unit[28]

It is the sudden increase of APC current $I_z^{(s)}(\pi)$ at a higher bias $V_b = 0.6$ V [inset of Fig. 2(a)] that led to the nonlinear bias dependence of STT. To understand the microscopic origin of this sudden increase, we plot spin-resolved transmission coefficient versus electron energy E (relative to the Fermi energy E_F) in Fig. 3, calculated at $V_b = 0.75$V. The ↑ or ↓ denotes the majority or minority spin channel in the left Fe lead. For APC, the ↑ channel of the left lead transmits to the ↓ channel of the right lead through the MgO. Figure .3 shows that there is an abrupt increase in ↑ channel transmission at about $E = 0.3$ eV. For a symmetric MTJ, roughly half V_b is dropped at each Fe/MgO interface. Hence the abrupt increase of transmission at $E \approx 0.3$ eV should contribute to APC current when the bias $V_b = 0.6$ V. This is indeed what is found [inset of Fig .2(a)]. We conclude that the sudden increase of $I_z^{(s)}(\pi)$ is due to the abrupt increase of the ↑ channel transmission, which, importantly, is also due to bias-dependent transport features as we explain now.

The inset (a) of Fig.3 plots the transmission hot spot of APC(↑) in the two-dimentional (2D) BZ, which is the transverse momentum ($\mathbf{k}_{||}$) resolved transmission coefficient. There is a clear bright ring surrounding the Γ

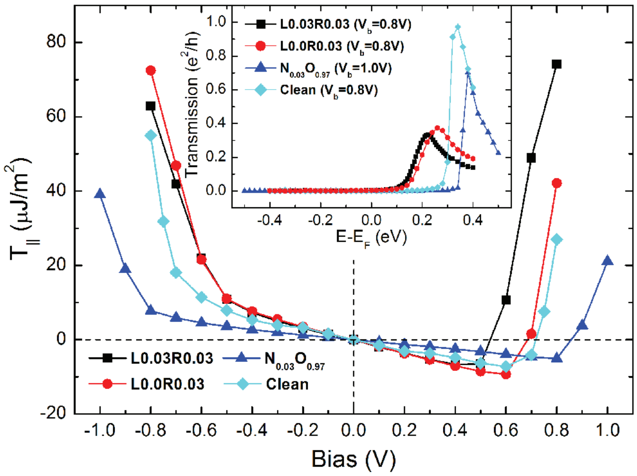

FIG. 4: (Color online) STT of Fe/MgO(7L)/Fe with oxygen vacancy disorder versus bias. LxRy denotes that there are x and y OVs at the left and right interface, respectively. $N_{0.03}O_{0.97}$ denotes that 3% oxygen atoms at both interfaces are replaced by nitrogen atoms.

point. The abrupt increase of the APC ↑ channel transmission is due to this bright ring. Focusing on one particular k point on this ring and scanning the electron energy, a single resonant peak is discovered in the transmission as shown in the inset (b) of Fig. 3.

Importantly, this sharp resonance is different from the well-known resonance states on Fe surfaces.[27] In particular, we found that this sharp APC resonance is only established at high bias and is located between the Δ_1 band in the left Fe and the $\Delta_5, \Delta_{2\prime}$ bands in the right Fe. The contribution of Δ_5 and $\Delta_{2\prime}$ bands to the total transmission is $k_{||}$ dependent, giving rise to the ring in the hot spot. A higher bias significantly changes the shape of the tunnel barrier: we checked that by artificially flattening the barrier potential from the biased slop shape, this sharp APC resonant channel disappears.

Actually, the existence of resonance is not only responsible for the sudden increase of STT but also responsible for the deviation of angular-dependent STT as shown in the inset (c) of Fig. 3. When at a resonant ring such as A point ($k_x = k_y = 0.278$ Å^{-1}), the angular-dependent in-plane STT deviates from a sine function and follows similar behavior as that in Fig. 2(c). When far from the resonant ring such as B point ($k_x = k_y = -1.624$ Å^{-1}), the angular dependent in-plane STT follows a sine function as well. Under most situations, at high bias, the resonance dominates the in-plane STT. Without resonant states, the Bloch wave should decay very fast in the tunnel barrier, the multiple scattering should be negligible, and Eq. 1 should hold in this case. However, in the presence of resonant states, the wave function of these states will decay little in the barrier and Eq. 1 is not valid anymore.

Having understood the microscopic physics behind the nonlinear bias dependence of STT, we note that the obtained threshold bias at $V_b \sim 0.6$ V for the *ideal* junction is higher than that reported experimentally,[6] which was about 0.3 V. Since experimental devices are never ideal, an investigation of defect scattering and its effect on STT is warranted. There are several possible defects such as oxygen vacancy in MgO, interfacial roughness,[15] material imperfections, etc. It was reported experimentally that due to compressive strain during crystal growth, oxygen vacancies (OV) are accommodated in MgO.[29] Both theory[20] and experiment[30] have shown that existence of OV can drastically influence spin-polarized transport and its effect on STT is therefore expected.

We calculated the in-plane STT from Eq. (1) by putting OVs in the interfacial MgO layer immediately adjacent to Fe. An alloy model $O_{1-x}Va_x$ is used, where Va stands for vacancy and x is the OV concentration. The disorder average is carried out by the NVC theory[18] mentioned above. Results are plotted in Fig. 4 versus V_b, and several observations are in order.

First, at low V_b, $T_{||}$ is linear for both disordered ($x \neq 0$) and clean samples ($x = 0$)—hence, the linear regime is not qualitatively altered by OVs. Second, both symmetric junctions where the same OV concentration is on both Fe/MgO interfaces (black curve with solid squares), and asymmetric junctions where OVs only exist at one Fe/MgO interface (red curve with solid circles), yield almost the same $T_{||}$. In particular, its slope $\tau_{||} \equiv dT_{||}/dV \approx -5.5 \times 10^{13}\tau_o$. This value is only slightly larger than that of the ideal junction, which has $\tau_{||} = -4.7 \times 10^{13}\tau_o$. Hence, a small amount of OV (e.g. 3%) does not alter $T_{||}$ significantly. These results should be compared to the experimental value of the slope $\tau_{||} = -3.2 \times 10^{13}\tau_o$ measured at $V_b = \pm 0.3$ V.[16] Giving the uncertainties in comparing our atomic structure to the experimental one, the quantitative consistency of our results is quite satisfactory. Third, in Ref. 20, it was shown that filling the OVs with nitrogen atoms can significantly reduce disorder-induced diffusive scattering and drastically increase the TMR ratio. Here, filling the OVs with N using the alloy model $O_{1-x}N_x$, we found that the $T_{||}$ is somewhat decreased, namely, its slope $\tau_{||} = -1.9 \times 10^{13}\tau_o$ (blue curve with up-triangles).

Similar to the ideal junction, systems with OV also show abrupt increase of $T_{||}$ at higher bias, which, we found, is also due to the quantum resonance in the 2D BZ discussed above. Different from the ideal case, existence of OVs shifts the threshold bias of $T_{||}$ to lower values thus bringing it closer to the experimental result.[6] As shown in the inset of Fig. 4, the effect of OV on $T_{||}$ can also be understood by investigating transmission of the ↑ channel in APC.

The OVs induce two new effects. First, interfacial OVs broaden the area having high transmission values in the hot spots and also suppress the transmission peak from 1.0 e^2/h to about 0.35 e^2/h (at 3% OV on both interfaces). The overall effect is to enhance $T_{||}$ slightly. Second, interfacial OVs shift the resonant peak in the ↑ channel of APC to lower energy and, as a result, the threshold bias is now shifted to lower values.

Remarkably, from Fig. 4 one can determine which Fe/MgO interface dominates STT. When OVs exist at both interfaces (black curve with solid squares), the threshold bias shifts to lower values from those of the clean sample for both V_b polarity. When OVs exist only at the right Fe/MgO interface (red curve with solid circles), the threshold bias shifts to lower value only in the negative V_b. When OVs are filled by N atoms (blue curve with up-triangles), the threshold bias shifts to higher V_b for both polarities.

Quantitatively, the threshold bias is $\sim$0.45V in the presence of 3% OV at interface. It is consistent with the experimental value $\sim$0.4 V (see Ref.[16]) with a 1.25-nm (6-ML) MgO barrier. A more recent experiment measured a threshold bias $\sim$0.2 V (see Ref.[8]) with a 1.0-nm (5-ML) MgO barrier. The experimentally measured resistance is 1.5 $\Omega\mu\text{m}^2$ also close to our calculated value for a junction with a 5-ML MgO barrier.

The effects of OVs on the out-of-plane STT are also very important. We have examined a junction using the wave-function-matching method. The calculation was done in a 7×7 lateral supercell containing five randomly distributed OVs at each Fe-MgO interface (thus $x \sim 10\%$). For $V_b = 0.5$ V and $E = E_F + 0.25$ eV, the calculated in-plane and out-of-plane STT are $20.30 \times 10^{14}\tau_o$ and $7.32 \times 10^{14}\tau_o$, respectively. These values are larger than that of the ideal junction which are $1.06 \times 10^{14}\tau_o$ and $0.94 \times 10^{14}\tau_o$ for in-plane and out-of-plane STT, respectively. The larger in-plane and out-of-plane STT in the 10% OV sample is attributed to the resonant tunneling discussed above. These results indicate that the interfacial OV disorder is not detrimental to the value of the out-of-plane STT. In comparison, interface roughness disorder quenches the out-of-plane STT as reported in Ref. 15.

IV. SUMMARY

In summary, the bias dependence of STT was investigated from atomic first principles, covering both low- and high-bias regimes. STT shows weak and linear bias dependence at small V_b but strong and nonlinear dependence at higher V_b. The angle dependence of STT is symmetric at low bias but asymmetric at high bias. The nonlinear behavior is marked by a threshold bias in the STT versus bias curve and is controlled by a resonant transmission channel in APC. Very importantly, disorder scattering by small amount of oxygen vacancies in MgO lowers the STT threshold bias but not the STT value, suggesting that the nonlinear STT can be tuned by clever interfacial engineering as also reported in Ref. 30 where crystal-growth temperature changes the OV contents.

V. ACKNOWLEDGEMENTS

K.X. thanks financial support by the National Basic Research Program of China (973 Program) under grant No. 2011CB921803 and NSF-China grant No. 10634070; H.G. thanks NSERC of Canada, FQRNT of Quebec, and CIFAR.

---

[1] J. C. Slonczewski, J. Magn. Magn. Mater. **159**, L1 (1996); L. Berger, Phys. Rev. B **54**, 9353 (1996).

[2] Z. Diao, D. Apalkov, M. Pakala, Y. Ding, A. Panchula, and Y. Huai, Appl. Phys. Lett. **87**, 232502 (2005).

[3] Z. Diao, A. Panchula, Y. Ding, M. Pakala, S. Wang, Z. Li, D. Apalkov, H. Nagai, A. Driskill-Smith, L.-C. Wang, E. Chen, and Y. Huai, J. Appl. Phys. **99**, 08G510 (2006); K. Yagami, A. A. Tulapurkar, A. Fukushima, and Y. Suzuki, *ibid.* **97**, 10C707 (2005).

[4] R. Matsumoto, A. Fukushima, K. Yakushiji, S. Yakata, T. Nagahama, H. Kubota, T. Katayama, Y. Suzuki, K. Ando, S. Yuasa, B. Georges, V. Cros, J. Grollier, and A. Fert, Phys. Rev. B **80**, 174405 (2009).

[5] J.C. Sankey, Y.-T. Cui, J. Z. Sun, J. C. Slonczewski, R. A. Buhrman, and D. C. Ralph, Nat. Phys. **4**, 67 (2008).

[6] H. Kubota, A. Fukushima, K. Yakushiji, T. Nagahama, S. Yuasa, K. Ando, H. Maehara, Y. Nagamine, K. Tsunekawa, D. D. Djayaprawira, N. Watanabe, and Y. Suzuki, Nat. Phys. **4**, 37 (2008).

[7] A. M. Deac, A. Fukushima, H. Kubota, H. Maehara, Y. Suzuki, S. Yuasa, Y. Nagamine, K. Tsunekawa, D. D. Djayaprawira, and N. Watanabe. Nat. Phys. **4**, 803 (2008).

[8] C. Wang, Y.-T. Cui, J. A. Katine, R. A. Buhrman, and D. C. Ralph, Nature Physics (2011) DOI: doi:10.1038/nphys1928, advance online publication 27 February 2011.

[9] S. C. Oh, S. Y. Park, A. Manchon, M. Chshiev, J. H. Han H.-W. Lee, J.-E. Lee, K.-T. Nam, Y. Jo, Y.-C. Kong, B. Dieny, and K.-J. Lee, Nat. Phys. **5**, 898(2009).

[10] I. Theodonis, N. Kioussis, A. Kalitsov, M. Chshiev, and W. H. Butler, Phys. Rev. Lett. **97**, 237205 (2006).

[11] A. Kalitsov, M. Chshiev, I. Theodonis, N. Kioussis, and W. H. Butler, Phys. Rev. B **79**, 174416 (2009).

[12] J. Xiao, G. E. W. Bauer, and A. Brataas, Phys. Rev. B **77**, 224419 (2008).

[13] M. Wilczyński, J. Barnaś, and R. Świrkowicz, Phys. Rev. B **77**, 054434 (2008).

[14] A. Manchon, N. Ryzhanova, A. Vedyayev, M. Chschiev, and B. Dieny, J. Phys.: Condens. Matter **20**, 145208 (2008).

[15] C. Heiliger, and M. D. Stiles, Phys. Rev. Lett. **100**, 186805 (2008).

[16] C. Wang, Y.-T. Cui, J. Z. Sun, J. A. Katine, R. A. Buhrman, and D. C. Ralph, Phys. Rev. B **79**, 224416 (2009).

[17] J. Taylor, H. Guo, and J. Wang, Phys. Rev. B **63**, 245407 (2001).

[18] Y. Ke, K. Xia, and H. Guo, Phys. Rev. Lett. **100**, 166805 (2008).

[19] S. Wang, Y. Xu, and K. Xia, Phys. Rev. B **77**, 184430

(2008).

[20] Y. Ke, K. Xia, and H. Guo, Phys. Rev. Lett. **105**, 236801 (2010).

[21] W. H. Butler, X.-G. Zhang, T. C. Schulthess, and J. M. MacLaren, Phys. Rev. B, **63**, 054416 (2001). J. Mathon, and A. Umerski, *ibid.* **63**, 220403 (2001).

[22] S. Yuasa T. Nagahama, A. Fukushima, Y. Suzuki, and K. Ando, Nat. Mater. 3, 868 (2004) 871.

[23] J. Faure-Vincent, C. Tiusan, E. Jouguelet, F. Canet, M. Sajieddine, C. Bellouard, E. Popova, M. Hehn, F. Montaigne, and A. Schuhl, Appl. Phys. Lett. **82**, 4507 (2003).

[24] S. S. P. Parkin, C. Kaiser, A. Panchula, P. M. Rice, B. Hughes, M. Samant, and S.-H. Yang, Nat. Mater. 3 (2004) 862.

[25] There is about 20% difference in the in-plane STT between the two methods at higher bias 0.8V.

[26] J. C. Slonczewski, Phys. Rev. B **39**, 6995 (1989).

[27] O. Wunnicke, N. Papanikolaou, R. Zeller, P. H. Dederichs, V. Drchal, and J. Kudrnovsky, Phys. Rev. B **65**, 064425(2002); P. X. Xu, V. M. Karpan, K. Xia, M. Zwierzycki, I. Marushchenko, and P. J. Kelly, *ibid.* **73**, 180402(R) (2006).

[28] Note, $1.0J \cdot V^{-1}m^{-2} = 3.038 \times 10^{18}\frac{\hbar}{2e}k\Omega^{-1}m^{-2}$.

[29] P. G. Mather, J. C. Read, and R. A. Buhrman, Phys. Rev. B **73**, 205412 (2006).

[30] G. X. Miao, Y. J. Park, and J. S. Moodera, Phys. Rev. Lett. **100**, 246803 (2008).